JOURNAL OF MATERIALS SCIENCE **35** (2000) 179–189

Precipitation sequence of various kinds of metastable phases in Al-1.0mass% Mg_2Si-0.4mass% Si alloy

K. MATSUDA
Department of Materials Science and Engineering, Faculty of Engineering, Toyama University, 3190, Gofuku, Toyama-shi, Toyama, 930, Japan
E-mail: matsuda@eng.toyama-u.ac.jp

Y. SAKAGUCHI*, Y. MIYATA‡
Toyama University, 3190, Gofuku, Toyama-shi, Toyama, 930, Japan

Y. UETANI
Research Institute for Technology, Toyama Prefectural University, 5180, Kurokawa, Kosugi, Imizu-gun, Toyama, 939-03, Japan

T. SATO, A. KAMIO
Department of Metallurgical Engineering, Faculty of Engineering, Tokyo Institute of Technology, 2-12-1, O-okayama, Meguro-ku, Tokyo, 152, Japan

S. IKENO
Department of Materials Science and Engineering, Faculty of Engineering, Toyama University, 3190, Gofuku, Toyama-shi, Toyama, 930, Japan

The precipitation of three new types of metastable phases, i.e., TYPE-A, TYPE-B and TYPE-C, with different crystal structures from the β' phase is proposed from our research on the change in crystal structures and formation sequence of metastable phases during the aging of the Al-1.0mass% Mg_2Si-0.4mass% Si alloy by a combination of analytical high resolution electron microscopy and energy dispersive X-ray spectroscopy. The sequence of their formation is explained as follows. First, precipitation of the β' phase and TYPE-B precipitate, then β' dissolution into the matrix and degradation of the TYPE-B precipitate. Finally, predominant precipitation of the metastable TYPE-A precipitate. The TYPE-C precipitate appeared heterogeneously in the over-aged condition.

1. Introduction

The addition of Si in excess to the Al-Mg_2Si alloys is well recognized to cause refined precipitates [1]. It has been suggested that the metastable phase of the alloys has the same crystal structure as the β' metastable phase. It is not well understood whether the addition of Si in excess also causes a change in the crystal lattice system of the metastable phases. An previously reported the crystal structure of the β' metastable phase is hexagonal having the lattice parameters of $a = 0.407$ nm and $c = 0.405$ nm in an Al-1.0mass% Mg_2Si alloy (the balanced alloy) based on the results of high resolution transmission electron microscopy (HRTEM), electron diffraction and energy dispersive X-ray spectroscopy (EDS) analysis [2, 3]. In the Al-1.0mass% Mg_2Si-0.4mass% Si alloy (excess Si alloy), it has been found that three new types of metastable phases that have different HRTEM images characteristics their of the β' phase in the balanced alloy. Also the lattice parameters and crystallographic orientation relationships between the two new types of metastable phases have been reported [4, 5]. The morphological changes and the amounts of those metastable phases with aging have not yet been investigated.

In this work, we have analyzed the crystal structures of the three new type of metastable phases in the excess Si alloy using HRTEM and EDS techniques and clarified the precipitation sequences of the new types of metastable phases for the first time in this type of alloy.

2. Experimental

An Al-1.0mass% Mg_2Si-0.4mass% Si (the excess Si) alloy was prepared using 99.99% pure aluminum, 99.9% pure magnesium and 99.9% pure silicon ingots. The ingots obtained were then hot- and cold-rolled

Present address: *Chuou-Hatsujo Co., Ltd., 68, Narumi, Midori-ku, Nagoya, 458, Japan; ‡Fujikoshi Co. Ltd., 3-1-1, Yoneda, Toyama-shi, Toyama, 930, Japan.

into 0.2 mm thick sheets. These sheets were solution treated at 848 K for 3.6 ks and quenched in chilled water. The aging treatment was performed at 523 K in a salt bath. The thin specimens for the HRTEM observation were prepared by the electrolytic polishing method and were observed using an EM-002B (TOPCON Co., Ltd.) transmission electron microscope operated at 200 kV. EDS analysis was performed using a TEM-ECON (EDAX Inc.) equipped with the EM-002B.

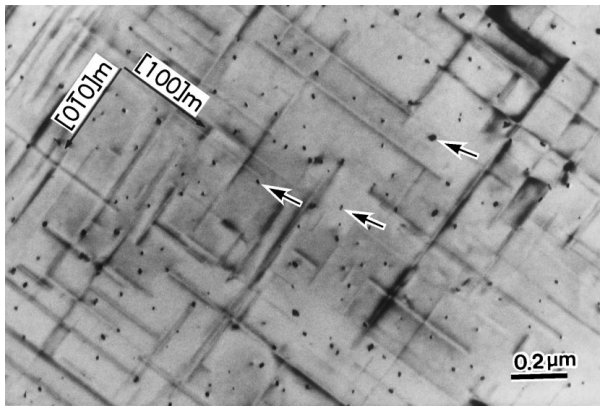

Figure 1 Transmission electron micrograph of an Al-1.0mass% Mg_2Si-0.4mass% Si alloy aged at 523 K for 12 ks. An incident beam direction is parallel to the [001]m matrix direction.

3. Results

The bright field image of the excess Si alloy aged at 523 K for 12 ks is shown in Fig. 1. A number of rod-shaped precipitates are observed to be aligned in the ⟨100⟩ directions of the matrix. The particle-like precipitates marked with the arrows are the rod-shaped precipitates located parallel to the [001]m direction of the matrix. We call them "edge-on" hereafter. Fig. 2 shows examples of the micro-beam diffraction (MBD) patterns obtained from the edge-on of precipitates for the specimen aged at 523 K for 60 ks. The MBD patterns of Fig. 2b–d were taken from the edge-on marked by ①, ② and ③ in Fig. 2a, respectively. The MBD patterns exhibit different arrangements of the diffraction spots. These MBD patterns were previously reported by Matsuda *et al*. [4, 5] . The metastable phases corresponding to the MBD patterns are designated as TYPE-A (Fig. 2d), TYPE-B (Fig. 2b) and TYPE-C (Fig. 2c) precipitates.

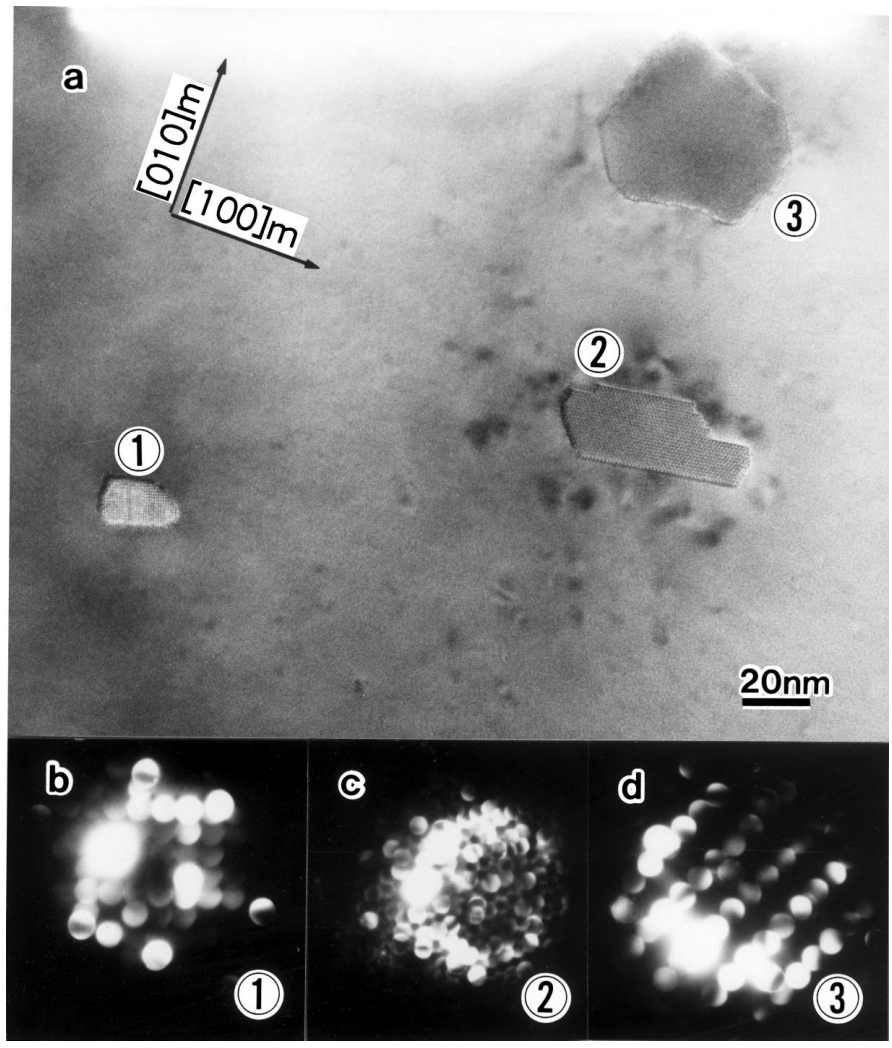

Figure 2 The bright field images of the cross-section of the precipitates in an Al-1.0mass% Mg_2Si-0.4mass% Si alloy aged for 60 ks. These precipitates indicate different micro-beam diffraction patterns from each other. Micro-beam diffraction patterns of (b), (c) and (d) correspond to the precipitates indicated in ①, ② and ③ in (a), respectively.

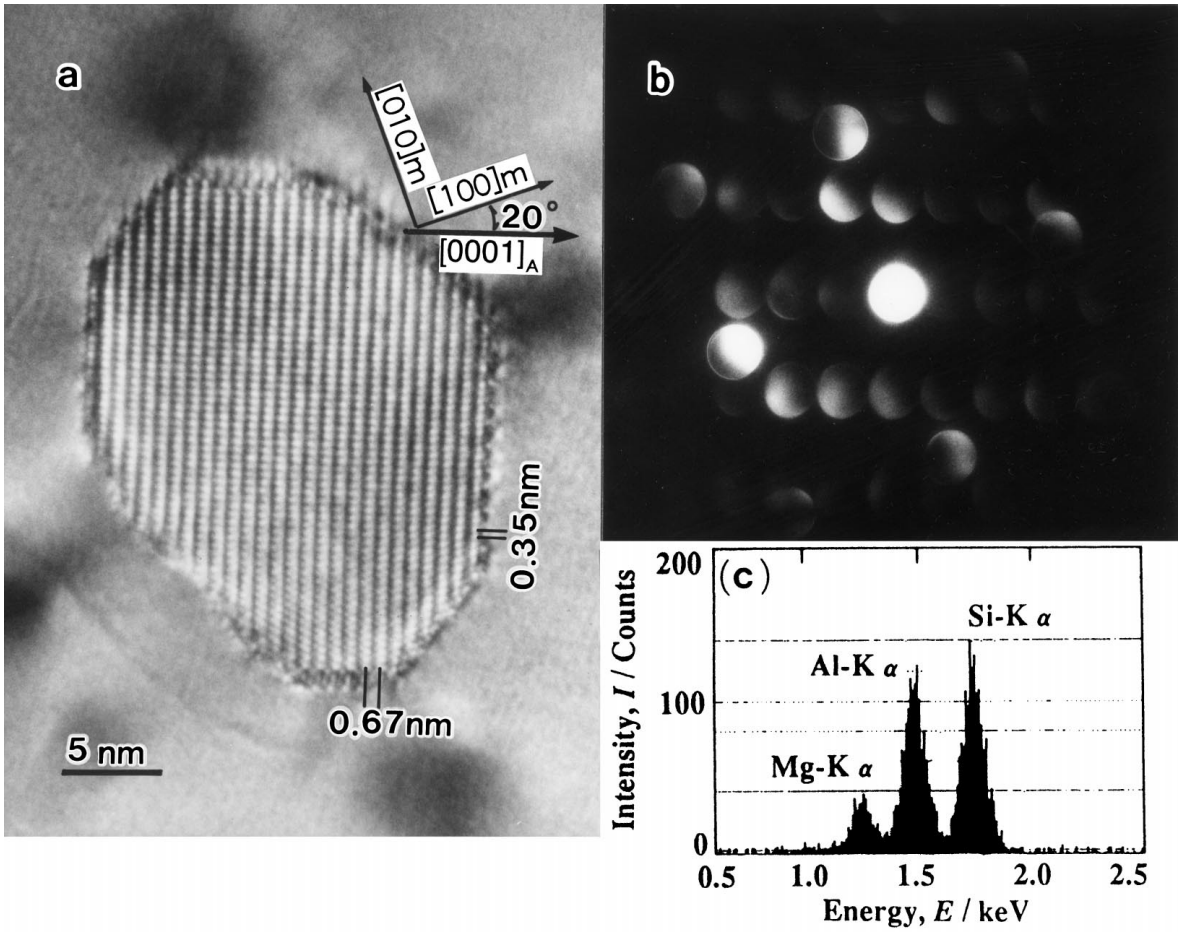

Figure 3 (a) A typical high resolution image of the TYPE-A precipitate in an Al-1.0mass% Mg_2Si-0.4mass% Si alloy aged at 523 K for 12 ks; (b) MBD pattern of (a) and (c) EDS profile of (a).

3.1. The TYPE-A precipitates

A typical high resolution image of the edge-on of the TYPE-A precipitate is shown in Fig. 3 together with the MBD pattern and EDS profile. The MBD pattern of Fig. 3b is similar to the one shown in Fig. 2d. The TYPE-A precipitate has a hexagonal lattice with the lattice parameters of $a = 0.405$ nm and $c = 0.67$ nm [4]. The four features which characterize this type of

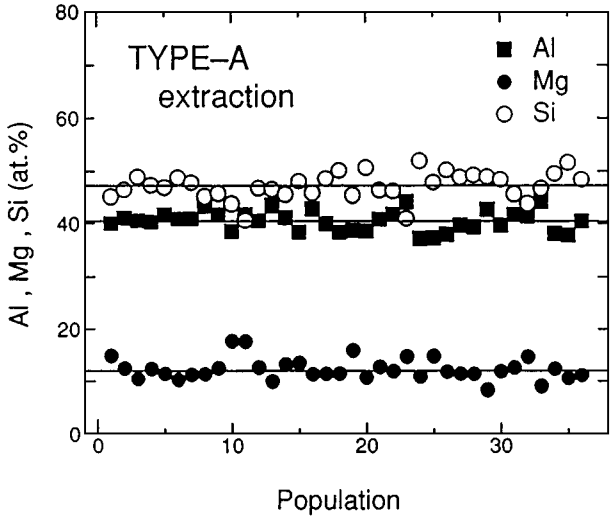

Figure 4 EDS analysis results for the TYPE-A precipitates extracted from the matrix by the thermal phenol method.

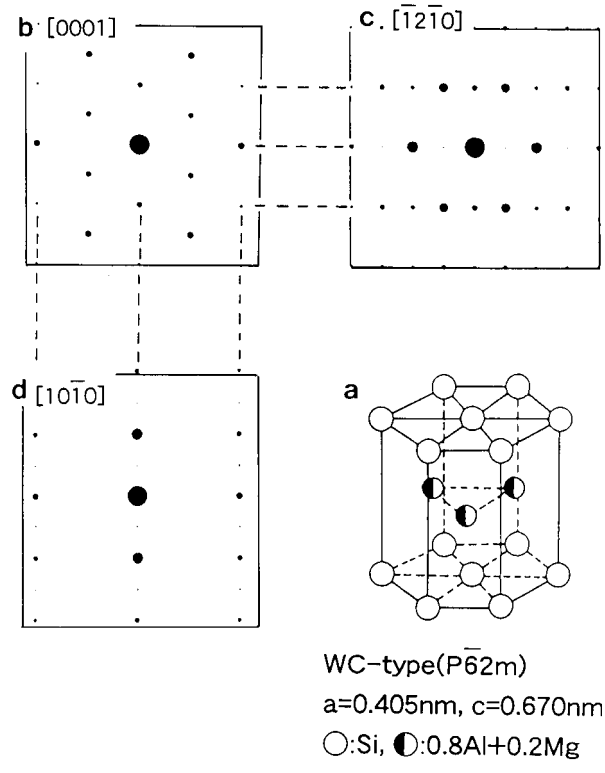

Figure 5 (a) Crystal structure of the TYPE-A precipitate and (b) to (d) calculated electron diffraction patterns for three directions of (a). (b), (c) and (d) correspond to the $[0001]_A$, $[\bar{1}2\bar{1}0]_A$ and $[10\bar{1}0]_A$ directions, respectively.

precipitate are as follows: (1) the shape is octagonal and has the largest diameter and length of all the metastable phases, (2) the bright dots in the edge-on of the HRTEM image indicate a rectangular arrangement with the length of the two sides being 0.35 and 0.67 nm, (3) the (1210) lattice plane of the TYPE-A precipitate is parallel to the (001)m matrix direction with an angle of 20° between the $[0001]_A$ and [100]m directions as shown in Fig. 3a, and (4) the peaks of Si and Al in the EDS spectra are higher than the Mg peak. In the case of Fig. 3c, the atomic ratio of Si/Mg = 3.71 is obtained. The TYPE-A precipitates were extracted from the matrix using the thermal phenol method to determine the accurate chemical composition of the TYPE-A precipitate in the present work. Fig. 4 shows the chemical compositions of Si, Al and Mg for various extracted precipitates. In Fig. 4, it is noted that the TYPE-A precipitate consists of 50 at % Si, 40 at % Al and 10 at % Mg. In our recent report, the EDS analysis was performed by the same method for an equilibrium Si precipitate for an over-aged condition in the excess Si alloy [6]. The result shows that no Al was detected in the Si precipitate extracted from the matrix, demonstrating the accuracy of the analysis on the extracted precipitates. Therefore, it is concluded that the TYPE-A precipitate consists of Si, Al and Mg. The averaged chemical composition was determined to be Si : Al : Mg = 5 : 4 : 1. From these investigations, the crystal structure of the TYPE-A precipitate is proposed as shown in Fig. 5a. Its fundamental lattice is hexagonal with the lattice parameters of $a = 0.405$ nm and $c = 0.67$ nm. The space group is P62m. Two atoms of Si are located on its basal plane and three atoms of Al and Mg with a ratio of Al : Mg = 4 : 1 are located on its half plane. Fig. 5b shows the calculated electron diffraction patterns of the unit cell in Fig. 5a. These calculated diffraction patterns are in good agreement with the experimental diffraction patterns reported in our recent paper [4].

Fig. 6a shows an HRTEM image of the β' phase in the balanced alloy aged at 523 K for 12 ks. In this aging condition the β' phase was predominant in the balanced alloy [2], while a small number of precipitates of the β' phase were observed in the excess Si alloys. The characteristic features of the HRTEM image of the β' phase is as follows [3]: (1) bright dots in the edge-on exhibit a hexagonal network with the spacing of 0.71 nm, (2) the hexagonal networks rotate around the

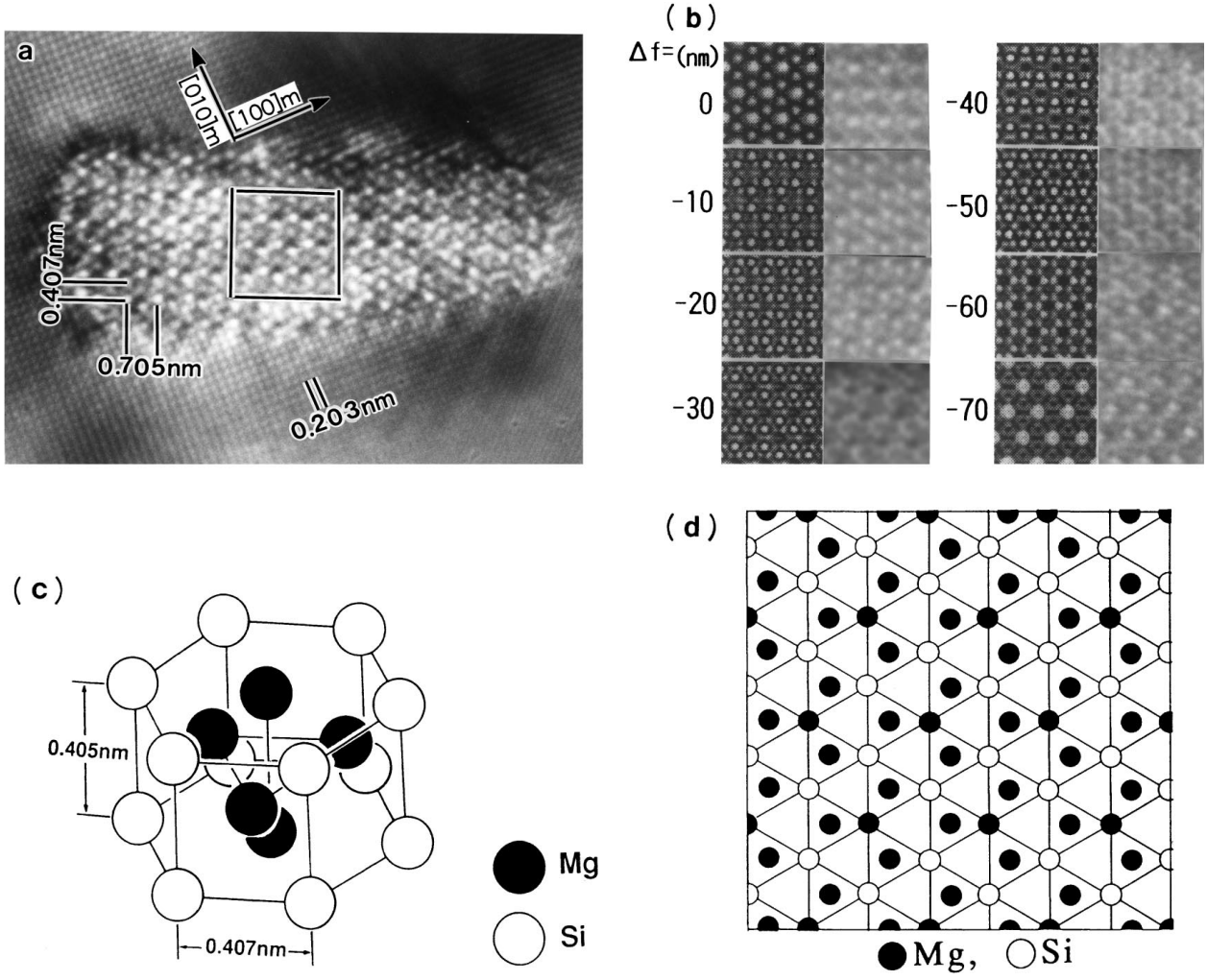

Figure 6 (a) A typical HRTEM image of the β' phase in an Al-1.0mass% Mg_2Si alloy aged at 523 K for 12 ks; (b) Changes in HR images with the amount of defocus (Δf). First and third columns show simulated HR images. Second and forth columns show obtained HR images. The thickness of the specimen used for simulation is 60.75 nm; (c) crystal structure of the β' phase [3]; (d) the projected potential for the unit cell of the β' phase parallel to the [0001] direction.

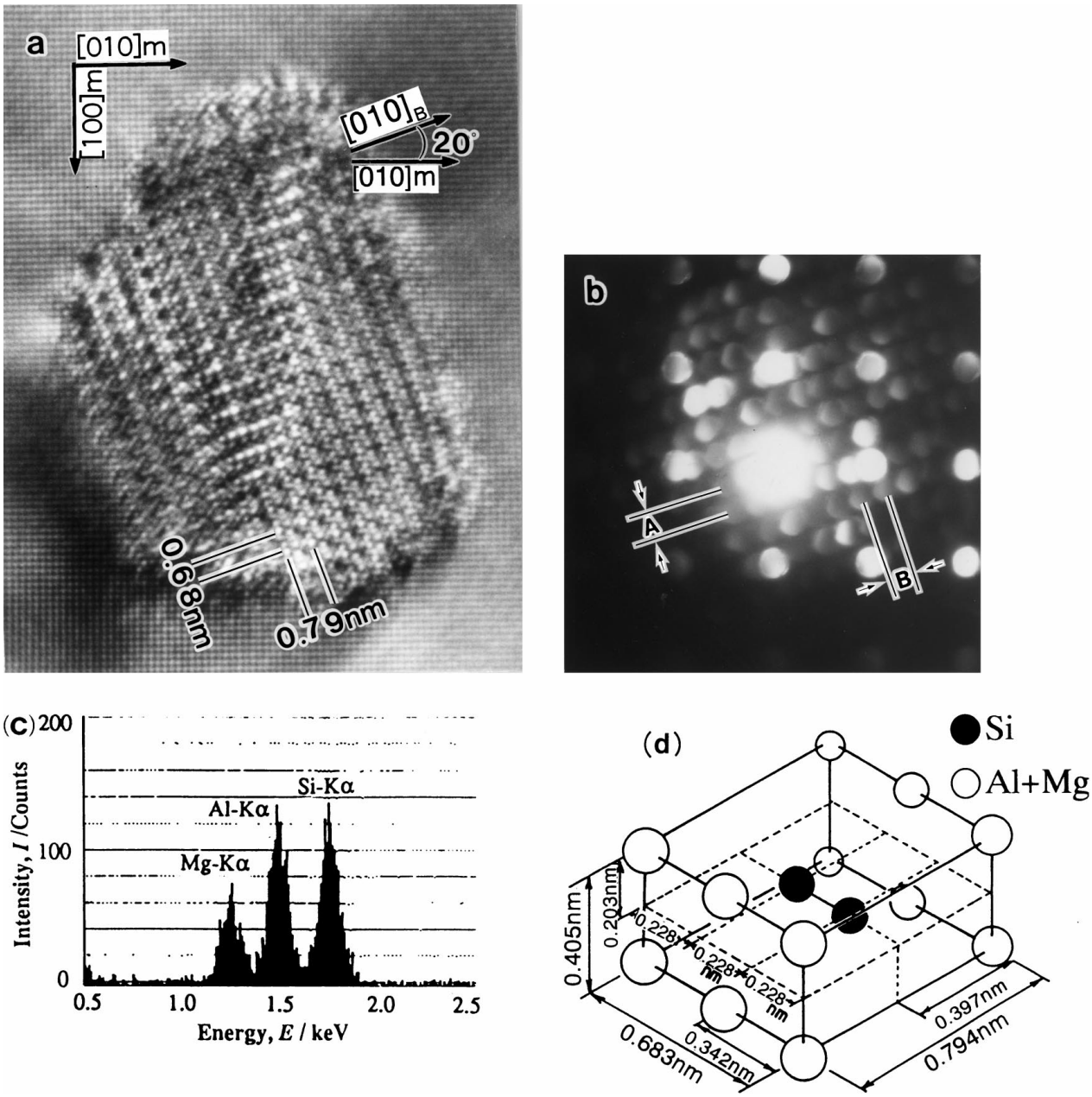

Figure 7 (a) A typical HRTEM image of the TYPE-B precipitate in an Al-1.0mass% Mg_2Si-0.4mass% Si alloy aged at 523 K for 12 ks; (b) MBD pattern of (a); (c) EDS profile of (a); and (d) crystal structure of the TYPE-B precipitate.

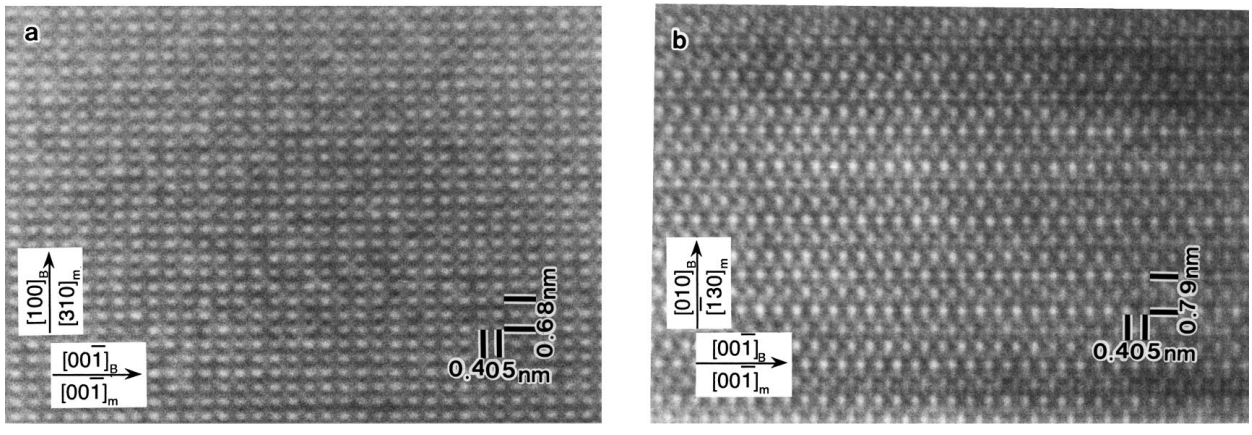

Figure 8 HRTEM images of the TYPE-B precipitates taken from the directions normal to their longitudinal directions. Incident beam directions are parallel to the [1̄30]m (a); and [310]m (b).

$[0001]_{\beta'}$ axis at various angles with the matrix. Fig. 6b shows the simulated HRTEM images for the atom arrangement with the crystal structure shown in Fig. 6c. As compared with the observed HRTEM image showing a surrounding square in Fig. 6a and the simulated image ($\Delta f = -20$ nm), both images are in good agreement with each other. Comparing the simulated images of Fig. 6b with the projected potential parallel to the [0001] direction for the unit cell of the β' phase shown in Fig. 6d, the columns of Mg atoms on the basal plane are brighter or darker than the columns of the other atoms for all defocus conditions. This is probably the reason why a hexagonal network of 0.705 nm is often observed in the HRTEM images of the edge-on of the β' phase [2, 3].

3.2. The TYPE-B precipitates

A typical HRTEM image of the TYPE-B precipitate, its MBD pattern and EDS profile are shown in Fig. 7. The rectangular arrangement of MBD disks in Fig. 7b is similar to that in Fig. 2b. The characteristic features of the TYPE-B precipitate observed in the HRTEM image is as follows [5]: (1) the shape is ellipsoid and a pair of its sides are parallel to each other, (2) the bright dots of the HRTEM images of its edge-on indicate a rectangular arrangement and the lengths of the two sides of this rectangle are 0.68 and 0.79 nm, (3) the (001) lattice plane of the TYPE-B precipitate is parallel to the (001)m direction and the angle between the $[010]_B$ and [010]m directions is 20° as shown in Fig. 7a, (4) the peaks of Si and Al in the EDS spectra are higher than the one of Mg. The EDS result of Fig. 7c gives the ratio of Si/Mg equal to 2.5. Fig. 8 shows the HRTEM images of the longitudinal direction of the TYPE-B precipitate. The incident beam directions are [130]m // $[010]_B$ (Fig. 8a) and [310]m // $[100]_B$ (Fig. 8b). Spacings of 0.405, 0.68 and 0.34 nm are observed in Fig. 8a and a bright dot is also observed in the center of the rectangle having two sides of 0.79 and 0.405 nm spacings in

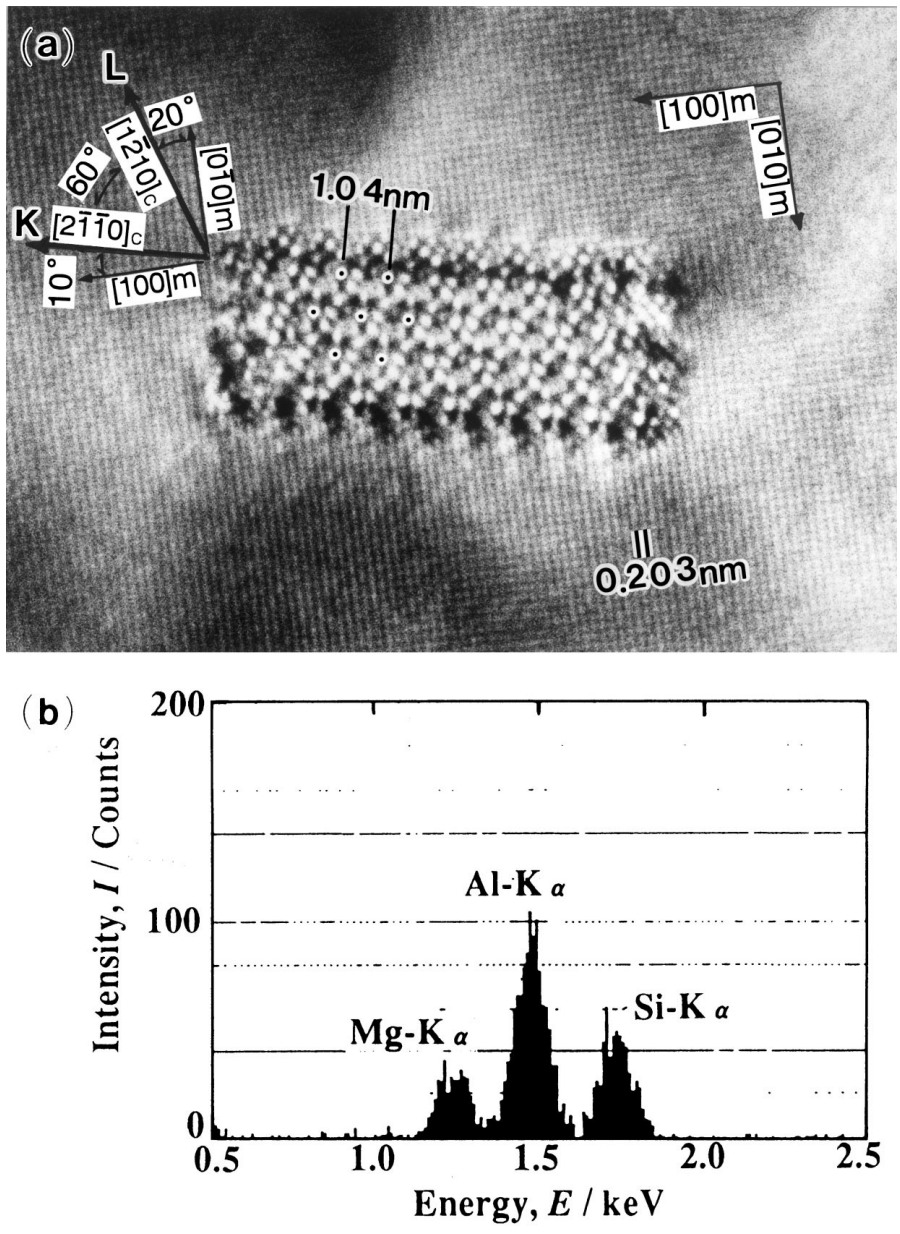

Figure 9 (a) A typical HRTEM image of the TYPE-C precipitate in an Al-1.0mass% Mg_2Si-0.4mass% Si alloy aged at 523 K for 12 ks; (b) EDS profile of (a).

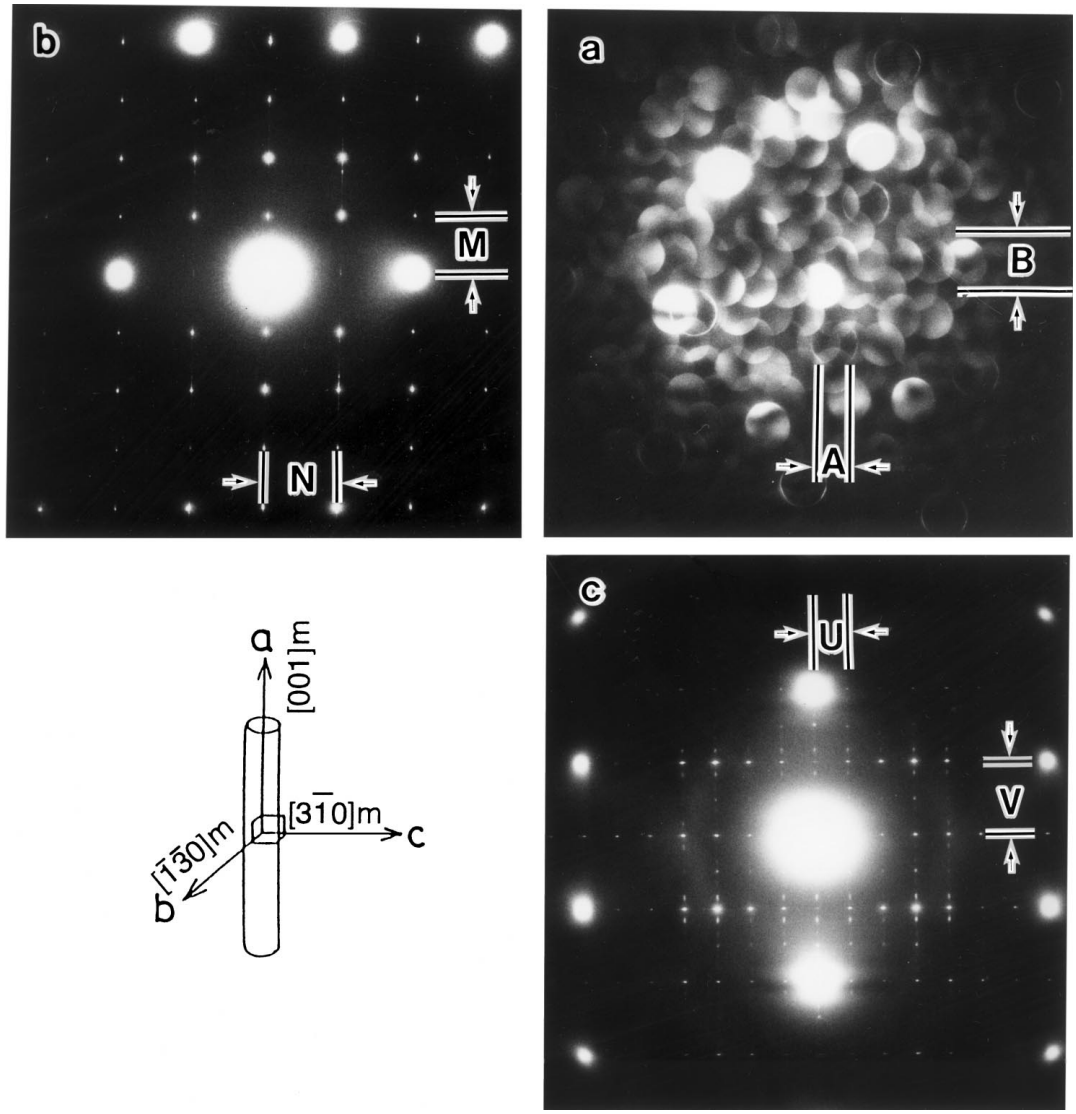

Figure 10 Electron diffraction patterns taken from three directions of the TYPE-C precipitate. (a) MBD pattern taken from the edge-on; (b) and (c) selected area diffraction patterns taken from the directions normal to the longitudinal directions of the TYPE-C precipitates.

Fig. 8b. The ratio of the chemical composition of the TYPE-B precipitate analyzed by the same thermal phenol method as shown in Fig. 4 is Si : Al : Mg = 5 : 4 : 2. The assumed atom positions in a unit cell of the TYPE-B precipitate is as follows: In Fig. 7d, the symbols ● and ○ represent the positions of Si (or 82% Si + 18% Al) and 64% Al + 36% Mg, respectively. Simulated electron diffraction patterns for several directions of the TYPE-B precipitate with the above unit cell are in good agreement with the observed ones reported in our recent paper [5].

3.3. The TYPE-C precipitates

A typical HRTEM image of the TYPE-C precipitate and its EDS profile are shown in Fig. 9. Small hexagonal networks of bright dots are observed inside the large hexagonal networks having a spacing of about 1.04 nm as shown in Fig. 9a. Both the Si and Mg peaks in the EDS spectrum are observed in this precipitate as shown in Fig. 9b and the estimated peak height ratio of Si/Mg is 1.22. In order to identify the crystal lattice of the TYPE-C precipitate, the electron diffraction patterns were obtained from the direction normal to the longitudinal direction using the same method as for the TYPE-A and TYPE-B precipitates. The angle between the K direction ([2$\bar{1}$10]c) of the TYPE-C precipitate and the [100]m direction is about 10°. On the other hand, the angle between the L direction ([1$\bar{2}$10]c) of the TYPE-C precipitate and the [010]m direction is about 20°, and is nearly equal to the angle of 18.4° between [010]m and [1$\bar{3}$0]m. Fig. 10 shows the selected area diffraction patterns taken of the TYPE-C precipitate. Fig. 10a represents the MBD pattern taken from the edge-on of the TYPE-C precipitate. Fig. 10b and c are selected area diffraction patterns taken of the directions normal to the longitudinal direction of the TYPE-C precipitate. The lattice plane spacings estimated from the spacings M and N in Fig. 10b are about 0.52 nm (about half the value of 1.04 nm obtained in Fig. 9a) and 0.405 nm (equal to the lattice constant of the Al matrix). The lattice plane spacings estimated from the spacings U and V in Fig. 10c are about 0.901 and 0.405 nm. If the crystal lattice of this precipitate is assumed to be hexagonal, having $a = 1.04$ nm, then the value of 0.52 nm must be equal to the spacing of

the $\{1\bar{2}10\}_C$ lattice plane and 0.901 nm is equal to the spacing of the $\{1\bar{1}00\}_C$ lattice plane. Based on these results, the crystal lattice of the TYPE-C precipitate is estimated as follows (see Fig. 11a): (1) it will be hexagonal having the lattice parameters of $a = 1.04 \pm 0.02$ nm and $c = 0.405$ nm. (2) The $(0001)_C$ lattice plane of the TYPE-C precipitate is parallel to (001)m and the angle between $[2\bar{1}\bar{1}0]_C$ and [100]m is 10°. Fig. 11b–d show simulated electron diffraction patterns for the crystal lattice of Fig. 11a. The arrangement of the diffraction spots and their spacings in Fig. 11b–d are in good agreement with those of Fig. 10a–c, respectively. Because of the limited number of extracted TYPE-C precipitates from the matrix using the thermal phenol method, the accurate chemical composition of the TYPE-C precipitate remains unknown. Therefore, the crystal structure of the TYPE-C precipitate is not yet fully determined in this study. A precipitate having the same lattice parameters as the TYPE-C precipitate was reported by Dumolt *et al*. [7] in the 6061 aluminum alloy. They called this precipitate the B′ phase, and speculated that the B′ phase is probably formed because of copper existing in the 6061 alloy. In the present work, it is clarified that the TYPE-C precipitate is one of the typical

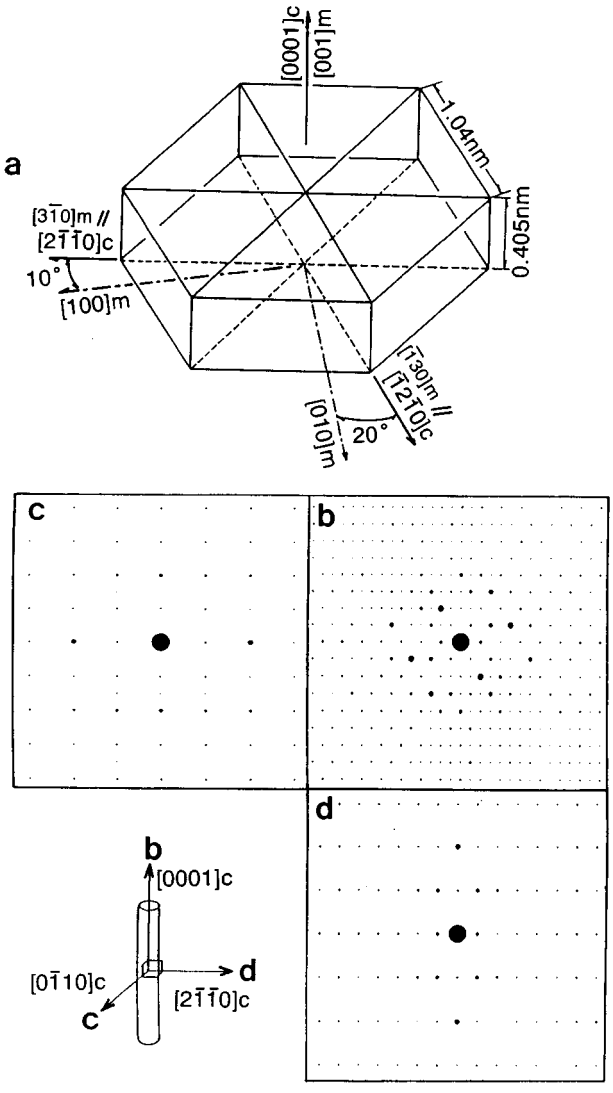

Figure 11 (a) A crystal lattice of the TYPE-C precipitate and (b) to (d) calculated electron diffraction patterns based on (a).

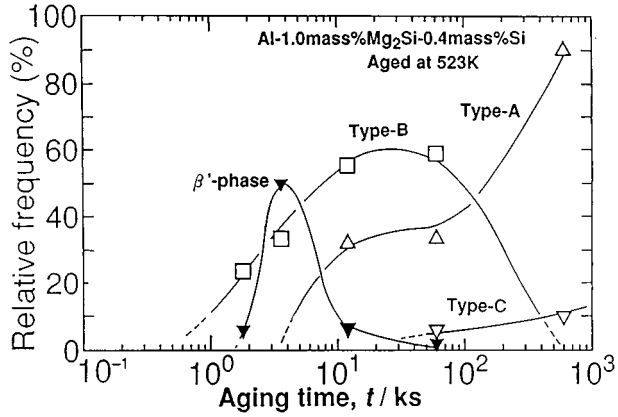

Figure 12 Changes in the relative frequencies of four types of metastable phases in an Al-1.0mass% Mg_2Si-0.4mass% Si alloy with aging time.

metastable phases in the excess Si alloy. Thus, the formation of the B′ phase in the 6061 alloy is caused by the excess Si of the 6061 alloy.

3.4. Effect of aging time

Fig. 12 shows the relative frequency of the amounts of four types of metastable precipitates. The β' phase is detected at the aging time of about 1.2 ks and its frequency increases rapidly to reach a maximum value, then rapidly decreases with prolonged aging. The β' phase disappeared after about 60 ks aging. The TYPE-B precipitates also appear after an aging time of 1.2 ks and then gradually increase with aging. During the early stage of aging, shorter than 3.6 ks, the total frequency of the β' phase and TYPE-B precipitates is lower than 100% because of the coexisting preliminary precipitates. Details of the preliminary precipitates which formed earlier will be reported elsewhere. The frequency of the TYPE-B precipitates increases up to 50% of all precipitates at 12 ks aging, then remains almost constant until 60 ks. After this, the frequency decreases and after 600 ks they disappear. The TYPE-A precipitates begin to appear when the frequency of the TYPE-B precipitates reaches its maximum value. A drastic increase in the frequency of the TYPE-A precipitate occurs correspondingly to the aging time when the frequency of the TYPE-B precipitate decreases. Finally, the TYPE-C precipitates appear at the aging time of 600 ks, although the frequency of the precipitates is the lowest among the four types of precipitates. The existence of this precipitation sequence has not been reported and has been clarified for the first time in the excess Si alloy by the present study.

4. Discussion

In the excess Si alloy, four types of metastable phases are progressively formed and compete against each other. Some of the phases are replaced by others. The disappearance of the β' phase in the excess Si alloy at a relatively early stage of aging seems to be unusual because the β' phase is predominantly formed in the

balanced alloy. In the balanced alloy, the β' phase has a sufficient stability even at the over-aging stage and coexists with the equilibrium β phase. The sequence of metastable phases based on our present results can be phenomenologically speculated as described next section. In the present work, the formation mechanism of the four types of the metastable phases are discussed.

4.1. β' phase, TYPE-B precipitate and TYPE-A precipitate

The β' phase is a predominant metastable phase in the balanced alloy. It is, therefore, assumed that the β' phase is more easily precipitated than any other metastable phase in this alloy system. Therefore, in the excess Si alloy, the β' phase will also be formed prior to any other metastable phase. It is well known that the equilibrium Mg_2Si and Si phases coexist in the region of excess Si on the Al-Mg-Si ternary equilibrium diagram. If the β'-phase is formed as a metastable phase having a chemical composition close to the equilibrium Mg_2Si, it can be expected that the Si-rich metastable phases of TYPE-A and TYPE-B precipitates are formed as a competing phase at the same time. In our recent report, the atomic ratio of Mg and Si in the β' phase is about Mg/Si = 1.68 [3], nearly equal to the equilibrium phase Mg_2Si, while

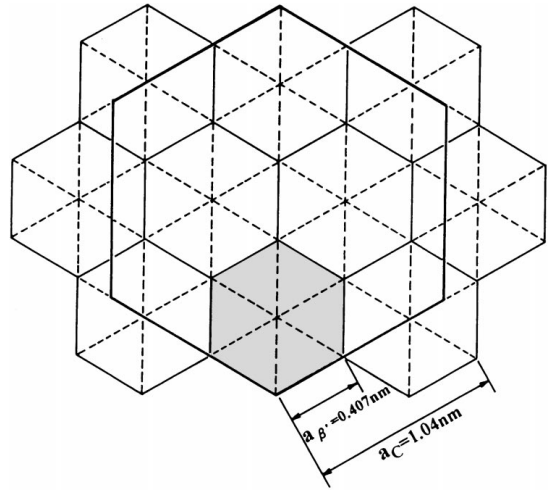

Figure 15 A crystallographic orientation relationship between the β' phase and the TYPE-C precipitate.

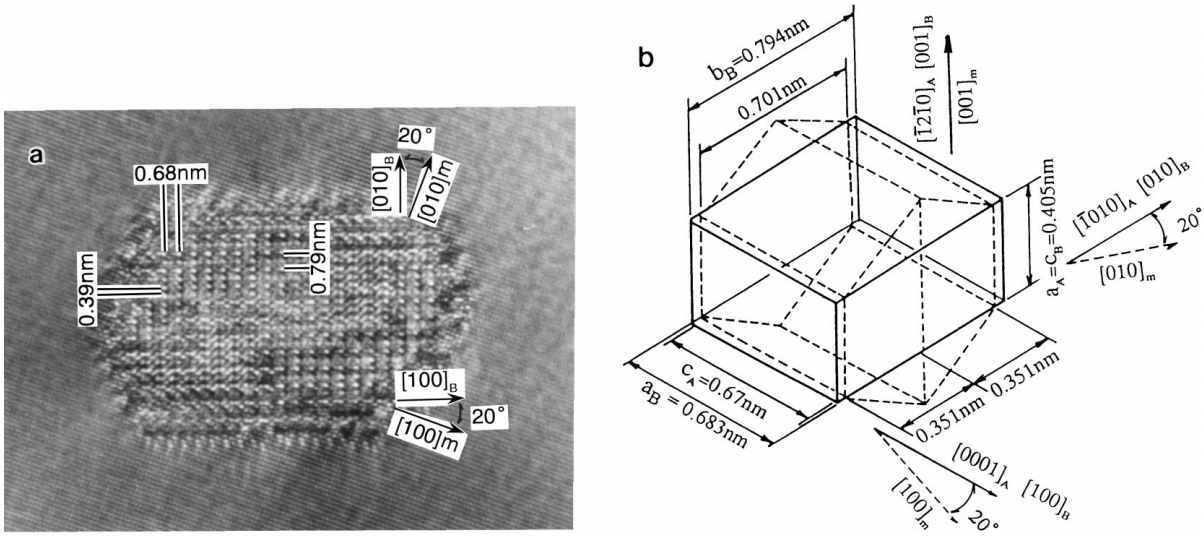

Figure 13 Relationships between the TYPE-A precipitate and the TYPE-B precipitate. (a) An HRTEM image of the rod-section of the TYPE-B precipitate; and (b) schematic illustration of the correspondence between the TYPE-A precipitate and the TYPE-B precipitate.

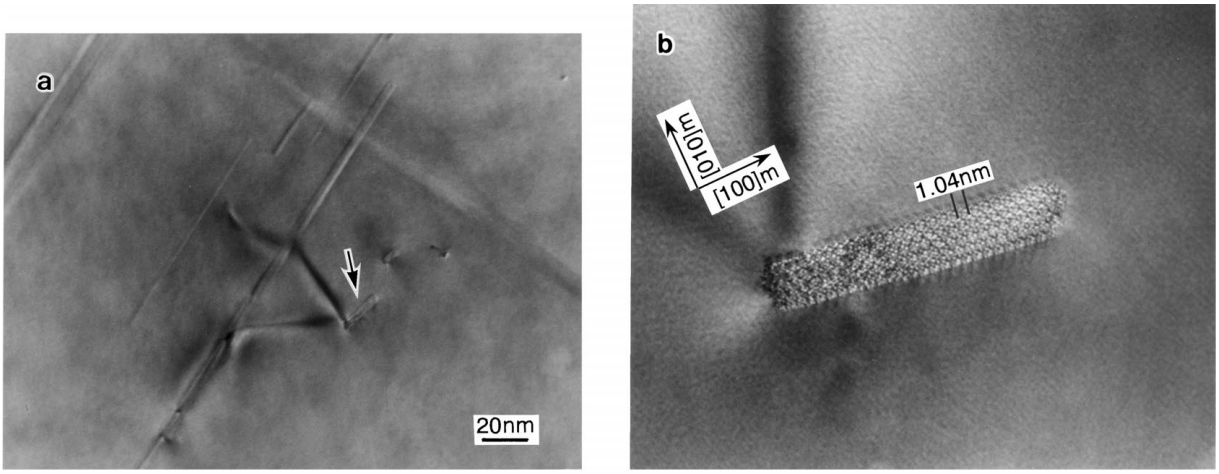

Figure 14 Heterogeneous nucleation of the TYPE-C precipitate in the specimen aged at 473 K for 120 ks after 10% deformation. (a) Bright field image; and (b) enlarged photograph of the rod-section marked by the arrow in (a).

the TYPE-B consists of ternary elements, i.e., Al, Mg and Si and its ratio is about Al : Mg : Si = 4 : 2 : 5. It is clear that the TYPE-B precipitate is a Si-rich precipitate and is considered as the competing precipitate for the β' phase. Actually both the β' phase and the TYPE-B precipitate appeared at the same time during aging, and the number and mean size of both phases increase with increased aging. As aging progresses, the amount of the β' phase increases to a maximum value then drastically decreases. The amount of the TYPE-B precipitate reaches almost a constant value at the beginning of its decrease in the β' phase. Moreover, TYPE-A precipitates begin to appear at a similar time. The formation of the TYPE-A precipitate is dependent on both of the decrease in the β' phase and saturation of the amount of the TYPE-B precipitate. The reason of the β' phase disappearance can be explained. In our previous study, it was speculated that the β' phase of the balanced alloy is not directly transformed into the equilibrium β-Mg_2Si. The equilibrium β-Mg_2Si phase is nucleated at other sites, independent of the β' phase. When the β phase nucleates and begins to grow, the β' phase decomposes and dissolves into the matrix. In the case of the excess Si alloy, if the β'-phase also decomposes in the same way as the balanced alloy, it is considered that the TYPE-A precipitate may be formed by absorption of the Si and Mg elements released from the decomposed β' phases. The TYPE-A precipitate also contains Al, Si and Mg and the atomic ratio of theses precipitates is about Al : Mg : Si = 4 : 1 : 5. Therefore, the deficient Si needed for the formation of the TYPE-A precipitate will be supplied from the matrix.

As shown in a previous report, the electrical resistivities of the excess Si alloys continuously decreased even during over-aging period. It was found in this investigation that the electrical resistivity decreased until reaching 100% of the TYPE-A precipitate. Based on this result, Si supplied from the matrix to the TYPE-A precipitates will continue until the end of formation of the TYPE-A precipitates. With further aging, the

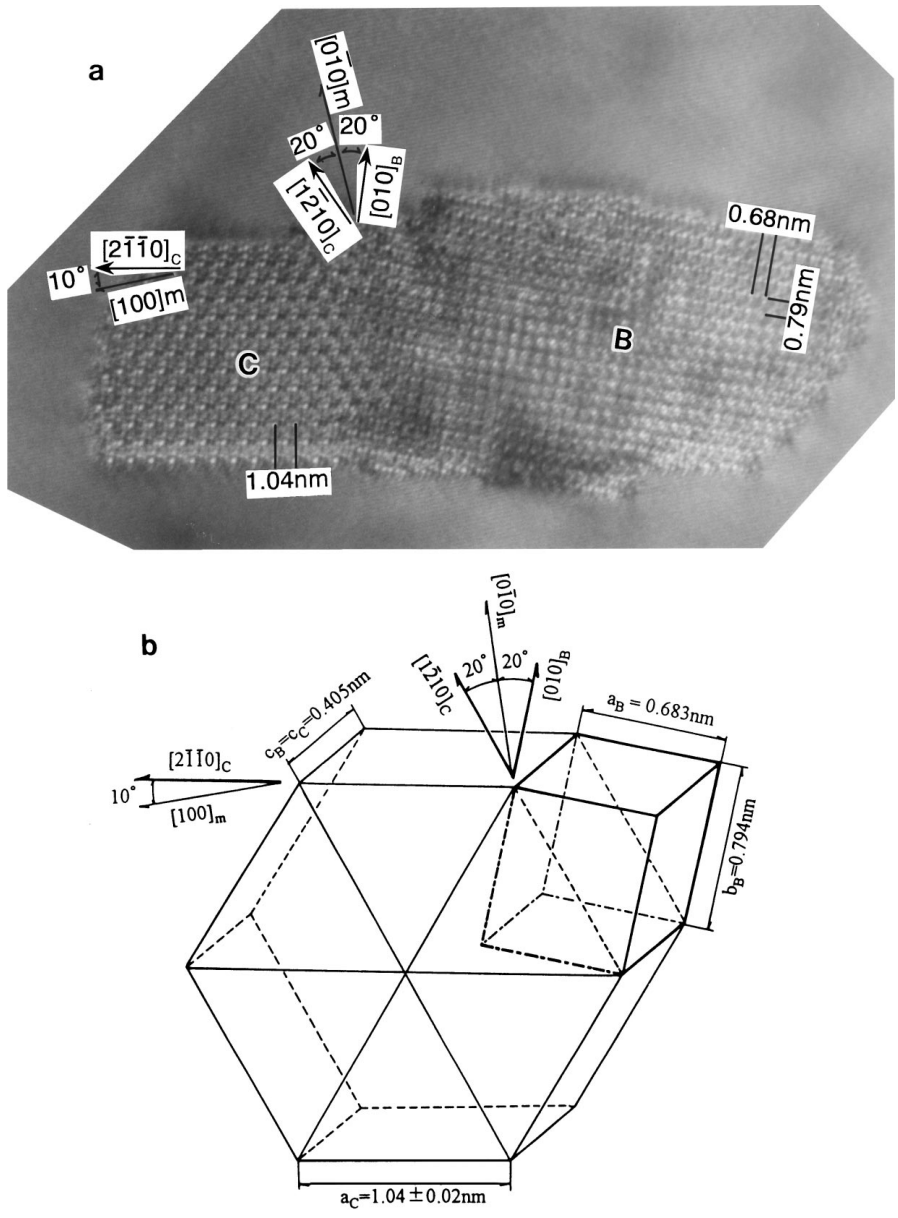

Figure 16 (a) An HRTEM image of the complicated rod-section. The region B is the TYPE-B precipitate and the region C is the TYPE-C precipitate; (b) a schematic illustration of the correspondence between the TYPE-B precipitate and the TYPE-C precipitate.

TYPE-A precipitate increases drastically instead of the disappearance of the β'-phase and the decrease of the TYPE-B precipitate. The transformation of the TYPE-B precipitate to the TYPE-A precipitate can then be understood. Fig. 13a is an HRTEM image of the edge-on of the TYPE-B precipitate. The arrangement of bright dots indicates a rectangular network with spacings of 0.68 and 0.79 nm. Otherwise, the spacing of 0.39 nm, which is nearly equal to one-half of 0.79 nm, is also observed. This spacing is close to 0.35 nm for the TYPE-A precipitate. As shown in the Fig. 13b, the size of the crystal lattice of the TYPE-A precipitate is similar to that of the TYPE-B precipitate. It is then predicted from a crystallographic analysis that the transformation of the crystal structure from the TYPE-B precipitate to the TYPE-A precipitate can easily occur. In this case, comparing the chemical composition of the TYPE-A precipitate and the TYPE-B precipitate, the Si content of the TYPE-A precipitate is more enriched than that of the TYPE-B precipitate. The Si supplied from the matrix is then needed for continuous formation of the TYPE-A precipitates. In this alloy system, a tendency can be seen that the phase consists of higher Si contents (or lower Mg contents) than the equilibrium β-Mg_2Si, and it appears at a later aging stage and is more stable.

4.2. The TYPE-C precipitate

The small amount of the TYPE-C precipitate appears at a relatively later aging stage. The precipitate has a tendency to heterogeneously nucleate as shown in Fig. 14. In these figures, the TEM image is of a specimen aged at 473 K, which corresponds to the maximum hardness just after 10% pre-deformation. Some coarse rod-shaped precipitates and dark string-like contrasts, which were introduced by predeformation, were observed in Fig. 14a. Fig. 14b shows an enlarged photograph of the rod-section indicated by the arrow in Fig. 14a. This edge-on of the precipitate indicates the same arrangement and the same spacing of the bright dots as that of the TYPE-C precipitate. The size of the a-axis of the TYPE-C precipitate is equal to 2.5 times that of the β' phase, as shown in Fig. 15. The chemical composition of the TYPE-C precipitate includes a greater Mg content than those of the TYPE-A and TYPE-B precipitates and is close to that of the β' phase. If the β' phase transforms to the TYPE-C precipitate, the β' phase must also absorb Si atoms from the matrix. There is the possibility of transformation from a TYPE-B precipitate to a TYPE-C precipitate, because the Si concentration of the TYPE-C precipitate is higher than that of the β'-phase and TYPE- C precipitates attached to the interface between the TYPE-B precipitate and the matrix were often observed as shown in Fig. 16a. In Fig. 16b, it is clearly shown that the length of the diagonal in the rectangle of the TYPE-B precipitate having two sides of 0.68 and 0.79 nm is about 1.04 nm, which is equal to the size of the a-axis of the TYPE-C precipitate. It is considered that the TYPE-C precipitate nucleates independently on the TYPE-A precipitate, because the crystal lattice and the ratio of Si/Mg in the TYPE-A precipitate is quite different from that of the TYPE-C precipitate.

5. Conclusions

The crystal structures of the three new types of metastable phases in an Al-1.0mass% Mg_2Si-0.4mass% Si alloy which are different from the β' phase in an Al-1.0mass% Mg_2Si alloy have been proposed based on the HRTEM observations and EDS analysis. The precipitation sequences of the four kinds of metastable phases were discovered in this alloy for the first time.

There are new types of metastable phases (TYPE-A, TYPE-B and TYPE-C) in an Al-1.0mass% Mg_2Si-0.4mass% Si alloy and they have different crystal structures from that of the β' phase. The atomic ratio of Mg and Si in the β' phase is about $Mg/Si = 1.68$, while the TYPE-A and the TYPE-B consist of the ternary elements Al, Mg and Si and their ratios are about $Al : Mg : Si = 4 : 1 : 5$ and $4 : 2 : 5$.

Both the β' phase and the TYPE-B precipitate appear at the same time during aging, then the amount and mean size of both phases increase with increased aging. As aging progresses, the amount of the β' phase increases to a maximum value then rapidly decreases, and the amount of the TYPE-B precipitate is almost a constant value.

With further aging, the increase in the TYPE-A precipitates rapidly occurs accompanied by a decrease in the TYPE-B precipitates after the disappearance of the β' phases and the termination of the new formation of the TYPE-B precipitate. A small account of the TYPE-C precipitates also heterogeneously appear in the matrix. The TYPE-A precipitate may disappear during the over-aged condition where the equilibrium β-Mg_2Si and Si phases are predominant.

Acknowledgement

The authors are grateful to the Hokuriku Fabrication Center of Shin-Nikkei Co., Ltd. for the chemical analysis of the alloys. Dr. K. Matsuda was partly supported by a grant from the Hokuriku Industrial Advancement Center.

References

1. M. KANNO, H. SUZUKI and Y. SHIRAISHI, *J. Japan Inst. Light Metals* **28** (1978) 553.
2. K. MATSUDA, S.TADA and S. IKENO, *J. Electron Microscopy* **42** (1993) 1.
3. K. MATSUDA, S. IKENO and S. TADA, *J. Japan Inst. Metals* **57** (1993) 1107.
4. K. MATSUDA, S. TADA, S. IKENO, T. SATO and A. KAMIO, *Scripta Met. Mater.* **32** (1995) 1175.
5. K. MATSUDA, S. IKENO, T. SATO and A. KAMIO, *Scripta Mater.* **34** (1996) 1797.
6. K. MATSUDA, S. TADA and S. IKENO, *J. Japan Inst. Metals* **58** (1994) 252.
7. S. D. DUMOLT, D. E. LAUGHLIN and J. C. WILLIAMS, *Scripta Met.* **18** (1984) 1347.

Received 12 December 1997
and accepted 15 July 1999